

## Two-Color Electric Field Resolved Transient Grating Spectroscopy of an Oligophenylenevinylene Dimer

Andrew M. Moran,<sup>1</sup> Jeremy B. Maddox,<sup>2</sup> Janice W. Hong,<sup>3</sup> Jeongho Kim,<sup>1</sup> Rene A. Nome,<sup>1</sup> Guillermo C. Bazán,<sup>3</sup> Shaul Mukamel,<sup>2</sup> Norbert F. Scherer<sup>1</sup>

<sup>1</sup>Department of Chemistry, The University of Chicago, Chicago, IL 60637, USA

<sup>2</sup>Department of Chemistry, The University of California at Irvine, Irvine, CA 92697, USA

<sup>3</sup>Department of Chemistry, The University of California at Santa Barbara, Santa Barbara, CA 93106, USA

E-mail: nfschere@uchicago.edu

**Abstract.** Two-color transient grating signals for an oligophenylenevinylene dimer and monomer are measured using spectral interferometry. It is shown that the spectral phases of the signals are particularly sensitive to nuclear dynamics and relaxation.

The introduction of diffractive-optics (DO) technology to femtosecond nonlinear spectroscopy experiments has allowed for heterodyned signal detection at optical frequencies with passively phase-stabilized interferometers.<sup>1</sup> The first DO-based transient grating (TG) experiments utilized wavelength-integrated heterodyne detection.<sup>2</sup> More recently, optical photon-echo spectra have been obtained for a variety of systems with spectral interferometry.<sup>3-5</sup> We have used spectral interferometry and TG spectroscopy in studies of chemical relaxation dynamics,<sup>6,7</sup> solute and solvent signal field resolution,<sup>8</sup> and high-frequency vibrational resonances by broadband coherent Raman emission.<sup>9</sup> The present work is a comparative study of nuclear relaxations dynamics for conjugated monomer and dimer systems.

The molecules considered here are a highly-symmetric paracyclophane linked oligophenylenevinylene dimer (5Rd) and its monomer constituent (5R) for which linear absorption spectra are given.<sup>6</sup> It should be noted that the spectra of our 510 and 550 nm probe pulses overlap with the fluorescence bands of 5R and 5Rd. These molecules do not absorb significantly at wavelengths longer than 500 nm in their ground states.

Details for our home-built, amplified 1 kHz Ti:Sapphire laser system and four-wave mixing interferometer are given elsewhere.<sup>6</sup> Pump pulses are produced by second harmonic generation in a 0.2 mm BBO crystal and are centered at 405 nm with 70 fs duration. Tunable probe pulses are generated with a home-built noncollinear optical parametric amplifier, which yields 25-35 fs pulses from 500-700 nm.

Spectrograms of the experimentally measured signal pulses are computed using

$$\Sigma(\omega, t) = \left| \int_{-\infty}^{\infty} d\tau E_s(\tau) g(\tau - t) \exp(-i\omega\tau) \right|^2, \quad (1)$$

where  $E_s(\tau)$  is the signal field and we take  $g(t - \tau)$  to be a gaussian function with a width equal to the probe pulse duration. In our notation,  $T$  is the experimentally controlled delay between the pump and probe pulses and  $t$  is absolute time, where  $t=0$  is defined as the time the peak of the probe pulse arrives at the sample.<sup>6</sup> Signal spectrograms for degenerate frequency experiments are presented in the top row of Figure 1. The signal emission times for 5R (5Rd) are  $t=11$  fs ( $t=10$  fs) and  $t=4$  fs ( $t=0$  fs) for pulse delays of  $T=0$  fs and  $T=500$  fs, respectively. Nuclear relaxation is taken to be complete at  $T=500$  fs because evolution of the signal spectrograms is not observed after  $T=200$  fs. Spectrograms for experiments with 510 nm probe pulses are presented in the middle row of Figure 1. The signal emission times for 5R (5Rd) are  $t=4$  fs ( $t=1$  fs) and  $t=-2$  fs ( $t=-3$  fs) for pulse delays of  $T=0$  fs and  $T=500$  fs, respectively. The signal field of 5Rd is more positively chirped at  $T=0$  than at  $T=500$  fs, whereas the time-frequency shape for 5R is insensitive to the pulse delay. Data collected with probe pulses centered at 550 nm are displayed in the bottom row of Figure 1. The signal emission times for 5R (5Rd) are  $t=-2$  fs ( $t=-3$  fs) and  $t=-4$  fs ( $t=-5$  fs) for pulse delays of  $T=0$  fs and  $T=500$  fs, respectively.

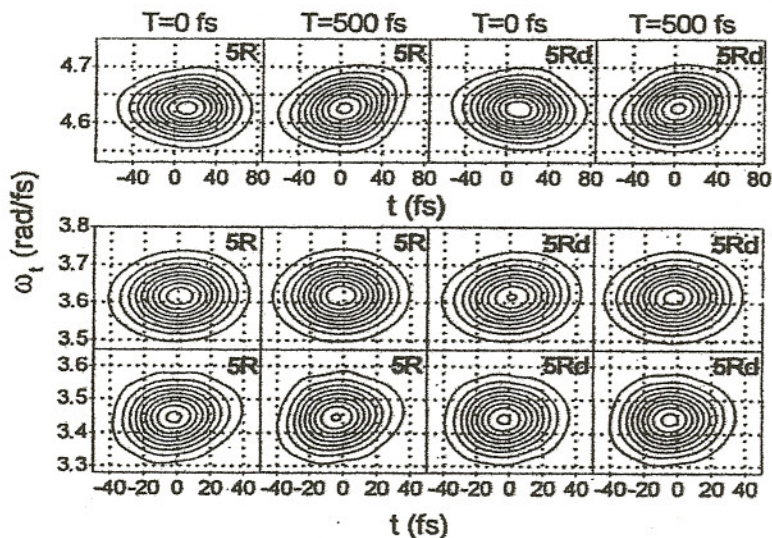


**Figure 1.** Spectrograms for 5R and 5Rd computed using Equation (1). The delay between the pump and probe pulses,  $T$ , is given at the top of each column. 70 fs pump and probe pulses centered at 405 nm were used to obtain the data in the first row. The data in the middle row were collected with 70 fs, 405 nm pump pulses and 30 fs, 520 nm probe pulses. Measurements in the bottom row were acquired with 70 fs, 405 nm pump pulses and 25 fs, 550 nm probe pulses. The chemical species is indicated in each panel.



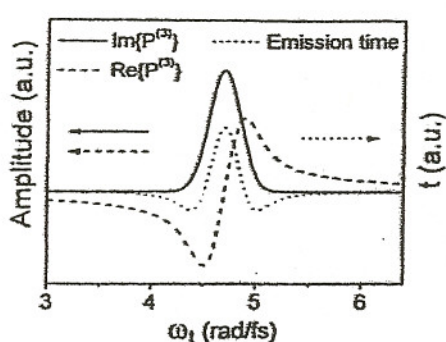


**Figure 2.** Absorptive (solid) and dispersive (dashed) projections of the nonlinear polarization. The emission time (dotted) is computed as the group delay with  $\text{Re}\{P^{(3)}\}$ .

bandwidth of the probe pulse spectrum through the dispersive component of the signal phase.

### Acknowledgments

This research was supported by the NSF (CHE 0317009 and NIRT ERC 0303389).

### References

1. G. D. Goodno, G. Dadusc, and R. J. D. Miller, *J. Opt. Soc. Am. B* **15**(6), 1791-1794 (1998).
2. G. D. Goodno, V. Astinov, and R. J. Dwayne Miller, *J. Phys. Chem. A* **103**, 10630-10643 (1999).
3. T. Brixner, J. Stenger, H. M. Vaswani, M. Cho, R. E. Blankenship, and G. R. Fleming, *Nature* **434**, 625-628 (2005).
4. T. Brixner, T. Mancal, I. V. Stiopkin, and G. R. Fleming, *J. Chem. Phys.* **121**, 4221 (2004).
5. M. L. Cowan, J. P. Ogilvie, and R. J. D. Miller, *Chem. Phys. Lett.* **386**, 184 (2004).
6. A. M. Moran, J. B. Maddox, J. H. Hong, J. Kim, R. A. Nome, G. C. Bazan, S. Mukamel, and N. F. Scherer, *J. Chem. Phys.* **124**, 194904 (2006).
7. A. M. Moran, S. Park, and N. F. Scherer, *J. Phys. Chem. B* (in press, 2006).
8. A. M. Moran, R. A. Nome, and N. F. Scherer, *J. Chem. Phys.* **125**, 031101 (2006).
9. A. M. Moran, R. A. Nome, and N. F. Scherer, *J. Phys. Chem. A* (submitted, 2006).

This qualitative model predicts that positive emission times of relatively large magnitudes should be observed when the probe frequency is tuned to the resonance frequency. In contrast, negative signal emission times with small magnitudes are obtained when the probe pulse is tuned to the wing of the resonance. The data presented in Figure 1 exhibit this behavior.

The greatest change in the signal emission time as a function of pulse delay is observed in the experiment with degenerate 405 nm pulses. This experiment is sensitive to nuclear motion in regions of coordinate space that exceed the